PL-TR-97-2014

FIRST PRINCIPLES AND APPLICATIONS-ORIENTED IONOSPHERIC MODELING STUDIES, AND WAVE SIGNATURES IN UPPER ATMOSPHERE DENSITY

Matthew W. Fox
Xiaoqing Pi
Jeffrey M. Forbes

Boston University
Center for Space Physics
725 Commonwealth Avenue
Boston, MA 02215

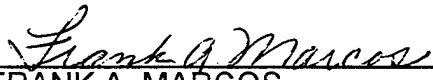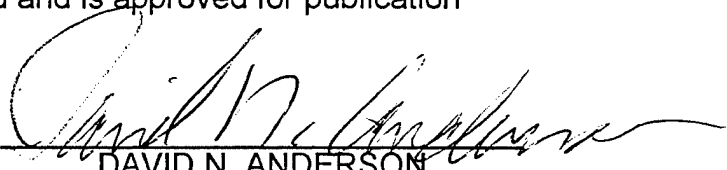January 1997

Scientific Report No. 3

PHILLIPS LABORATORY

Directorate of Geophysics

AIR FORCE MATERIEL COMMAND

HANSCOM AFB, MA 01731-3010

19970521 039

DTIC QUALITY INSPECTED 1

"This technical report has been reviewed and is approved for publication"

_____
FRANK A. MARCOS
Contract Manager

_____
DAVID N. ANDERSON
Branch Chief

_____
DAVID A. HARDY
Division Director

This report has been reviewed by the ESC Public Affairs Office (PA) and is releasable to the National Technical Information Service (NTIS).

Qualified requestors may obtain additional copies from the Defense Technical Information Center (DTIC). All others should apply to the National Technical Information Service (NTIS).

If your address has changed, or if you wish to be removed from the mailing list, or if the addressee is no longer employed by your organization, please notify PL/IM, 29 Randolph Road, Hanscom AFB, MA 01731-3010. This will assist us in maintaining a current mailing list.

Do not return copies of this report unless contractual obligations or notices on a specific document requires that it be returned.

REPORT DOCUMENTATION PAGE

Public reporting burden for this collection of information is estimated to average 1 hour per response, including the time for reviewing instructions, searching existing data sources, gathering and maintaining the data needed, and completing and reviewing the collection of information. Send comments regarding this burden estimate or any other aspect of this collection of information, including suggestions for reducing this burden, to Washington Headquarters Services, Directorate for Information Operations and Reports, 1215 Jefferson Davis Highway, Suite 1204, Arlington, VA 22202-4302, and to the Office of Management and Budget, Paperwork Reduction Project (0704-0188), Washington, DC 20503.

1. AGENCY USE ONLY (Leave blank)	2. REPORT DATE	3. REPORT TYPE AND DATES COVERED
	January 1997	Scientific No. 3

4. TITLE AND SUBTITLE
First-Principles and Applications-Oriented Ionospheric Modeling Studies and Wave Signatures in Upper Atmosphere Density

5. FUNDING NUMBERS

PE 63707F
PR 4026 TA GL WU MA

Contract
F19628-93-K-0012

6. AUTHOR(S)

Matthew W. Fox, Xiaoqing Pi, Jeffrey M. Forbes

7. PERFORMING ORGANIZATION NAME(S) AND ADDRESS(ES)

Boston University
Center for Space Physics
725 Commonwealth Avenue
Boston, MA 02215

8. PERFORMING ORGANIZATION REPORT NUMBER

9. SPONSORING/MONITORING AGENCY NAME(S) AND ADDRESS(ES)

Phillips Laboratory
29 Randolph Road
Hanscom AFB, MA 01731-3010

Contract Manager: Frank Marcos/GPIM

10. SPONSORING/MONITORING AGENCY REPORT NUMBER

PL-TR-97-2014

11. SUPPLEMENTARY NOTES

12a. DISTRIBUTION/AVAILABILITY STATEMENT

Approved for public release; distribution unlimited

12b. DISTRIBUTION CODE

13. ABSTRACT (Maximum 200 words)

The Phillips Laboratory Global Theoretical Ionospheric Model (GTIM) has formed the basis for a series of investigative studies. First, a multiple ion version of the theoretical code has been developed that is based on the same numerical solution type, to help insure that 0+ densities are consistent with the existing one-ion GTIM. Next, two new applications of the GTIM have been completed, in the study of wavelike disturbances in low-latitude electric fields, demonstrating the resulting wavelike ionospheric effects, and in a study to determine the F-region peak signatures that could be inferred from in situ measurements made at DMSP altitudes. Finally, a system for ionospheric raytracing is described that is based on a simple analytical profile model that can readily absorb real-time information and whose raytracing specification can be substantially improved with only minimal updates. Work performed on neutral density studies has concentrated on the delineation and interpretation of longitudinal structures in SETA data. These include the "longitude/UT" effect and longitudinal wave structures.

14. SUBJECT TERMS	15. NUMBER OF PAGES
Theoretical Ionospheric Modeling, Applications Modeling, Neutral Density Wave Signatures	40
	16. PRICE CODE

17. SECURITY CLASSIFICATION OF REPORT	18. SECURITY CLASSIFICATION OF THIS PAGE	19. SECURITY CLASSIFICATION OF ABSTRACT	20. LIMITATION OF ABSTRACT
Unclassified	Unclassified	Unclassified	SAR

NSN 7540-01-280-5500

Standard Form 298 (Rev. 2-89)
Prescribed by ANSI Std Z39-18

TABLE OF CONTENTS

Illustrations

The dotted line shows the same predictions made from the "ground-truth" ionosphere, shown in the right insert. The three lines above show the predictions made when Nmax is variously utilized in the propagation predictions at the circuit mid-point, end-points, and both, when SIMPLI parameters along the path are shifted only the zeroeth order. The three lines lying nearest to the dotted line are made when SIMPLI Nmax are refit along the whole path.

1. INTRODUCTION

The Phillips Laboratory Global Theoretical Ionospheric Model (hereafter, GTIM) has formed the basis for a series of investigative studies. First, a multiple ion version of the theoretical code has been developed that is based on the same numerical solution type, to help ensure that O^+ densities are consistent with the one-ion GTIM and that validation results obtained for the F-region will still be valid. Next, two new applications of the GTIM have been completed, in the study of wavelike disturbances in low-latitude electric fields and in a demonstration that the resulting ionospheric effects are also wavelike, and in a study to determine the F-region peak signatures that could be inferred from in situ measurements made at DMSP altitudes. Finally, a system for ionospheric raytracing is described that is based on a simple analytical profile model that can readily absorb real-time information and whose raytracing specification can be substantially improved with only minimal updates.

Work performed on neutral density studies has concentrated on the delineation and interpretation of longitudinal structures in the SETA data. These include the "longitude/UT" effect and longitudinal wave structures.

2. THE MULTIPLE-ION GTIM

One significant effort over this period has been the extension of the Phillips Laboratory GTIM to the solution of multiple ion species over a significantly greater range of altitudes. This has involved three major areas of development within the model:

- rewriting the equations of continuity and momentum for more than one ion, including both ion-ion and ion-electron interactions

- updating physical drivers for the model to permit reliable ion density derivations at much higher altitudes

- revising and updating reaction rates

The third area of development for the GTIM was principally undertaken at Computational Physics Inc. (hereafter, CPI) Boston and will not be discussed further in this report. The other two areas as they were performed at Boston University are discussed in the following two sections.

2.1 Deriving Ion Densities

The GTIM solution method for a one-ion formulation is described in Anderson (1973). Essentially, an expression for ion flux derived from the momentum equation is substituted into the continuity equation. This expanded continuity equation is then finite-differenced, and the resulting equation, that is tridiagonal in the ion densities (denoted N_i), is solved numerically along magnetic field lines, from the footpoint at 125 km in one hemisphere to the conjugate point in the other hemisphere.

We now consider the multiple ion situation. In the first instance, we form an equivalent expression for ion fluxes from the momentum equation for each of a number of ions. The momentum equations include terms from each of collisions with other ions (say, j) and with electrons. The electron momentum equation is used to eliminate the electric field term in the manner of the one-ion formulation, and the resultant expression for ion fluxes is of the same general form as that obtained for one ion, permitting the same substitution into the continuity equation and the same type of numerical solution. However, in three ways, the expression is more complex than the one-ion case:

- ion density and electron density are no longer equal, and N_i/N_e terms appear in the expression

- ion-ion interactions are included, and ion velocities become important to the solution as the relative velocities between ions define the momentum transfer

2

- ion-ion couplings for the ith ion also include coupling of the jth ion with electrons, owing to the electric field term in the momentum equation.

Thus, strictly speaking, the equation for ion flux is not linear in N_i. On the other hand, the higher order terms are generally small and can be arranged to appear only as modifiers to collision frequencies. Rearranging the higher order terms determining these effective collision frequencies are key steps in obtaining density solutions in the multiple ion GTIM.

We have thus outlined an approach for deriving ion densities for each of a number of different species. The ions required to define the ionosphere and plasmasphere are O^+, H^+ and He^+, and solutions are sought for each ion in turn at each time step. Because the ion densities are solved sequentially rather than simultaneously, much care is taken to ensure that ions are not artificially created or destroyed as numerical artifacts. This involves making adjustments to both production and loss rates and is best illustrated in an example.

Let us look at the O^+-H^+ charge exchange reaction and first consider the situation at an altitude of around 300 km. The loss rate (β) for O^+ due to this charge exchange amounts to typically 30% of the total O^+ loss rate, and thus, when this reaction is included in the calculations, model F-region O^+ densities drop by around 30%. However, at these low altitudes, no H^+ can be formed, owing to the rapid loss of H^+ through the reverse reaction. In this situation, the answer is to modify the forward loss rate by a factor that depends on the reverse loss rate (β_{REV}) and the time step (ΔT). We say that the fraction of O^+ that can be lost out of the amount one is trying to lose is the same as the fraction of H^+ that one is able to form over the time step, and that the rest charge exchanges rapidly back to O^+. Specifically, this fraction is $\exp(-\beta_{REV}\Delta T)$.

At a higher altitude (say, 1500 km), O^+-H^+ is primarily a source of O^+. One derives a production term (locally) for O^+ that goes as $\kappa \, n(H^+) \, n(O) \, \Delta T$. However, this production should not physically exceed the density of the available source terms (here H^+ and O,

3

mostly the latter being the smaller term at high altitudes). To ensure this, production rates are modified by a factor of $\exp(-\kappa \, n(H^+) \, \Delta T)$ to reflect the fraction of O that can be lost over the time step. It should also be noted that because both n(O) and $\beta_{REV}(H^+)$ are steeply varying functions of altitude, that the altitude profiles of these $\exp(-X \, \Delta T)$ terms are effectively step functions, and that the choice of how one averages these decay terms over the time step ($\exp(-X \, \Delta T)$ vs $\exp(-X \, \Delta T/2)$, say) has no influence on the final densities derived in the model.

2.2 Revising Model Drivers

As outlined above, each ion density can be derived from an expanded continuity equation (using effective ion fluxes), that becomes a tridiagonal matrix when finite-differenced. The coefficients that relate the adjacent terms in this matrix are dependent on a number of factors. Some of these factors are those that define the physical environment in which the ion density solutions are being derived, such as thermospheric densities and winds, electron and ion temperatures, and vertical **E x B** drifts. In the GTIM formulation, these physical quantities are not derived but are simply input, and are referred to as physical drivers for the (ionospheric) model.

Two important drivers have undergone recent revisions, specifically to address the issue of the higher altitudes being studied in the multiple ion GTIM.

First, vertical drifts have been generalized to include a variation with altitude. Most commonly this takes the form of using input values (based on Jicamarca radar or AE satellite observations) at low altitudes, tapering off above one input altitude to zero by a second input altitude. An additional term in the continuity equation resulting from the non-zero dV/dZ has been included. Furthermore, because this term can influence ion densities at the 10% level, the altitude dependence has been made smooth in the first derivative to avoid discontinuities in densities with altitude (runs at adjacent L-shells). A

4

tanh-like dependence is used. The input altitudes that define the vertical dependence were seen to vary with solar activity, and possibly other factors.

Next, the specification of electron and ion temperatures has been revised. Brace and Theis (1981) provided a convenient tabulation of a summary of measured Te at several altitudes (300 km, 400 km, 1400 km and 3000 km). At each location in the GTIM, a system has been set up that provides a smooth fit with altitude to the Brace and Theis values at that location, using a than-based functional form. The fit is further constrained by

- Te is set to the neutral temperature (from MSIS) at the fieldline base altitude (125km)

- Te being monotonic increasing with altitude at any location (not the same as monotonic increasing along the fieldline)

- Te being smoothly and slowly varying (larger rates of change lead to anomalously high ion velocities in the model that in turn lead to large density gradients amd sometimes numerical instabilities).

The second and third points mean that the fit will not necessarily pass through the Brace and Theis values, but will instead be a smooth fit guided by those values.

At higher altitudes than 3000 km, it is not sufficient to simply set Te to the 3000 km value. In filling the plasmasphere, the model is basically diffusing light ions up both hemispheres of a fluxtube until the pressure gradient term balances the gravity term (in the momentum equation). A flat Te profile above 3000 km would mean that much larger light ion densities are required at high altitudes to achieve this balance, and that the model refilling time is very long (tens of days). Above 3000 km, we have included a simple linear gradient in Te with altitude, and to avoid ion velocity related instabilities in the solution from steep temperature gradients, there is an additional transition region above 3000 km

5

where the Te gradient changes linearly with altitude from the 3000 km value to the input asymptotic value at a higher altitude (say, 4000 km).

The ion temperature, Ti, is derived from Te and T_N via a simple formulation of Banks and Kockarts that ensures a match with T_N at low ionization fraction, and Te at higher altitudes/fractions.

2.3 Testing Model Stability and Reliability

A couple of important issues regarding model stability and reliability have been recently addressed.

The first issue arises from the higher order terms in Ni that appear in the multiple ion momentum equation for the ith ion. There are different methods of rearranging the higher order terms to make the expression apparently linear in Ni to facilitate the GTIM solution for densities in the expanded continuity equation. Thus, it is important to show that the derived densities do not depend on the method of rearranging used.

The second issue arises from the use of ion fluxes from the momentum equation in the continuity equation, as it relies on collisions between species to define those fluxes. At sufficiently high altitudes, collisions are too rare, and artificial neutral atoms are added to achieve numerical stability. Thus, it is important to chronicle when these additional neutrals are required, and when they start to influence the densities derived.

Figure 1 demonstrates results obtained for ion densities at the apex of the L=3 fieldline for equinox, solar moderate conditions for a five day run. Each panel shows densities of each ion (and electrons) at a particular local time as a function of the logarithm of density of neutrals added. Flat lines thus indicate the desired insensitivity of the results to this numerical artifact. Adjacent panels show the same results using different methods of treating higher order terms in Ni, and the overall consistency of ion densities (to 10%

6
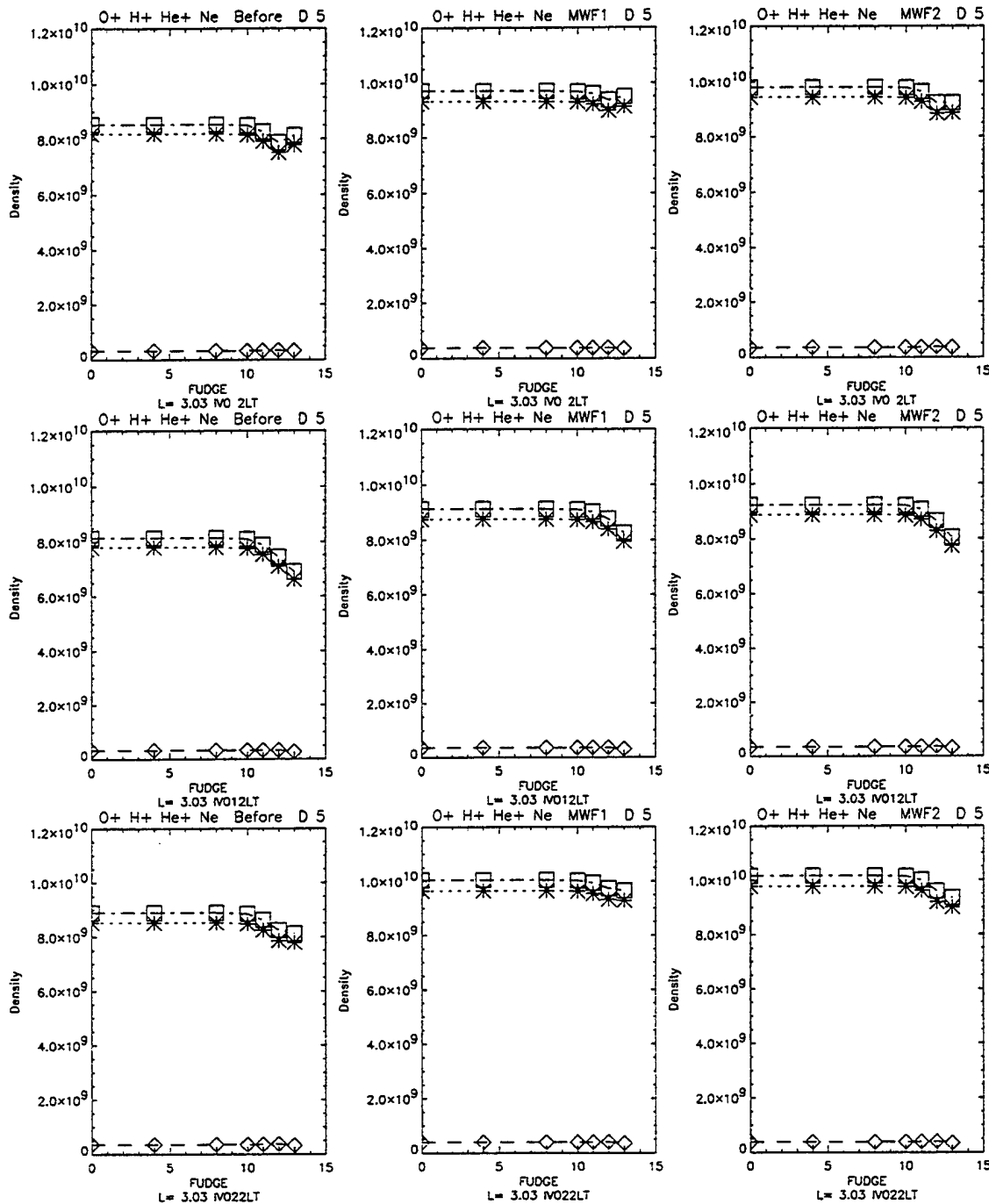
Figure 1. Electron (dot-dashed line) and ion densities (H^+ dotted, He^+ dashed, O^+ too small to be seen) at the apex of the L=3 fieldline for equinox, solar moderate conditions plotted as functions of the logarithm of density of artificially added neutral species, demonstrating reasonable insensitivity to that parameter. Panels side-by-side show the same results for different methods of linearizing the equation of continuity. Rows of panels correspond to results for 0200LT, 1000LT and 2200LT respectively, read from the top.

or so in this case) demonstrates insensitivity to the method. Other rows show the same behavior at other local times. The results are seen in Figure 1 to be encouraging at L=3. However, by L=4 the sensitivity to both neutrals and method is much more substantial (of the order of 50%), indicating that a different solution approach will be required at the highest altitudes in the plasmasphere.

At lower altitudes, reasonable agreement with observed ion densities has been obtained. Figures 2, 3 and 4 show comparisons of modeled profiles of O^+, H^+ and He^+ respectively, for selected local times against Arecibo ISR measured profiles from April 1995. In each panel, the different linestyles demonstrate the variations/uncertainties in the observations, while the symbols show the model results for consecutive run days. Overlapping symbols demonstrate convergence in the model densities, and qualitative and quantitative agreement with the observations is quite reasonable to 2000 km.

3. MODELING STUDIES - WAVELIKE DISTURBANCES

In an earlier report (Fox et al., 1994), the means by which the Phillips Laboratory GTIM at low latitudes was adapted to utilize vertical drift fields that include wavelike perturbations was outlined. Some preliminary results were also presented that included spurious effects at equatorial latitudes, whereby the wave-perturbed (or even default climatological) vertical drift field will cause the lowest L shells to drift below modeled altitudes and thus results could not be obtained for the complete period of a wave. More recent studies have remedied this problem, and a more exhaustive series of model runs under disturbed conditions has been conducted.

In the default configuration, the GTIM will terminate when an L-shell reaches a preset minimum altitude (around L=1.026) as the plasma drifts downward. In essence, the method currently employed is one that keeps track of how far below this minimum value the L
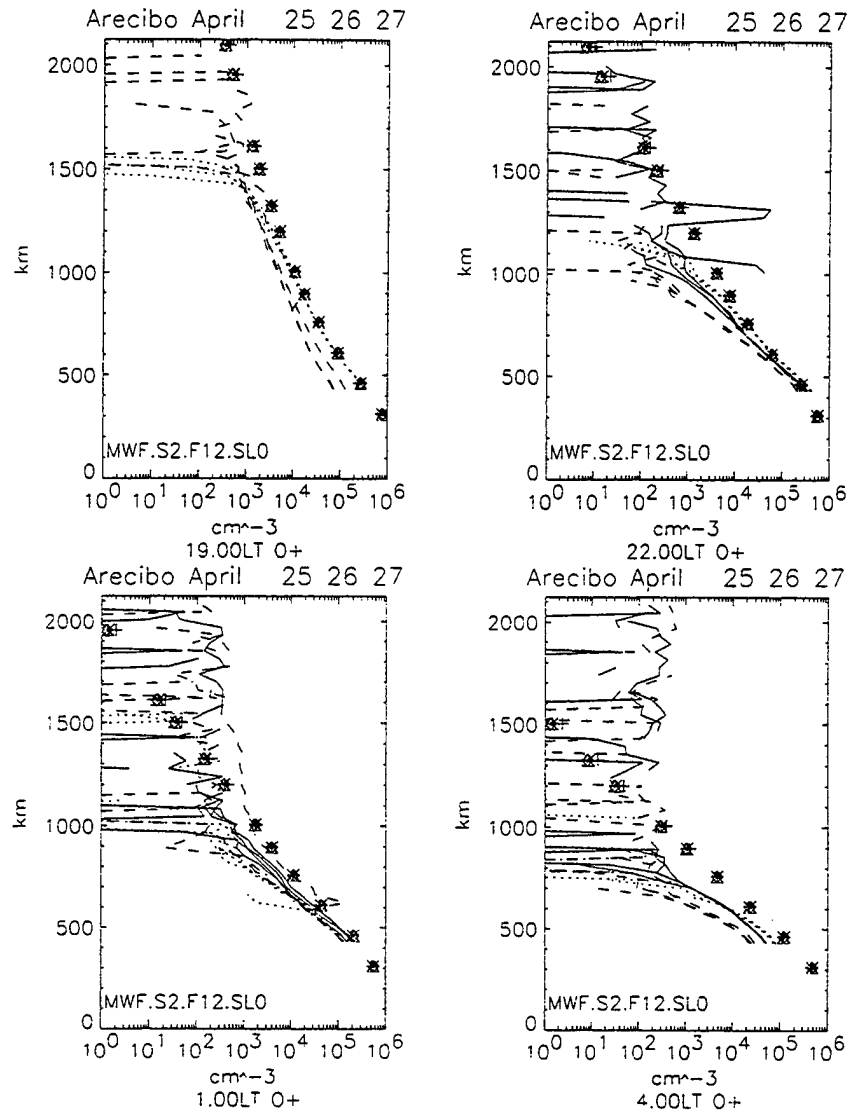
Figure 2. A comparison of modeled GTIM O^+ densities with observed profiles from the Arecibo, Puerto Rico, ISR. The four panels show comparisons at 1900LT, 2200LT, 0100LT and 0400LT. Observations are indicated by 25 April 1995 as solid lines, 26 April as dotted lines and 27 April as dashed lines. Overplots show radar observations made within 15 minutes. Symbols denote model densities for a 4-day simulation (day 1=plus, day 2=asterisk, day 3=diamond, day 4=triangle).
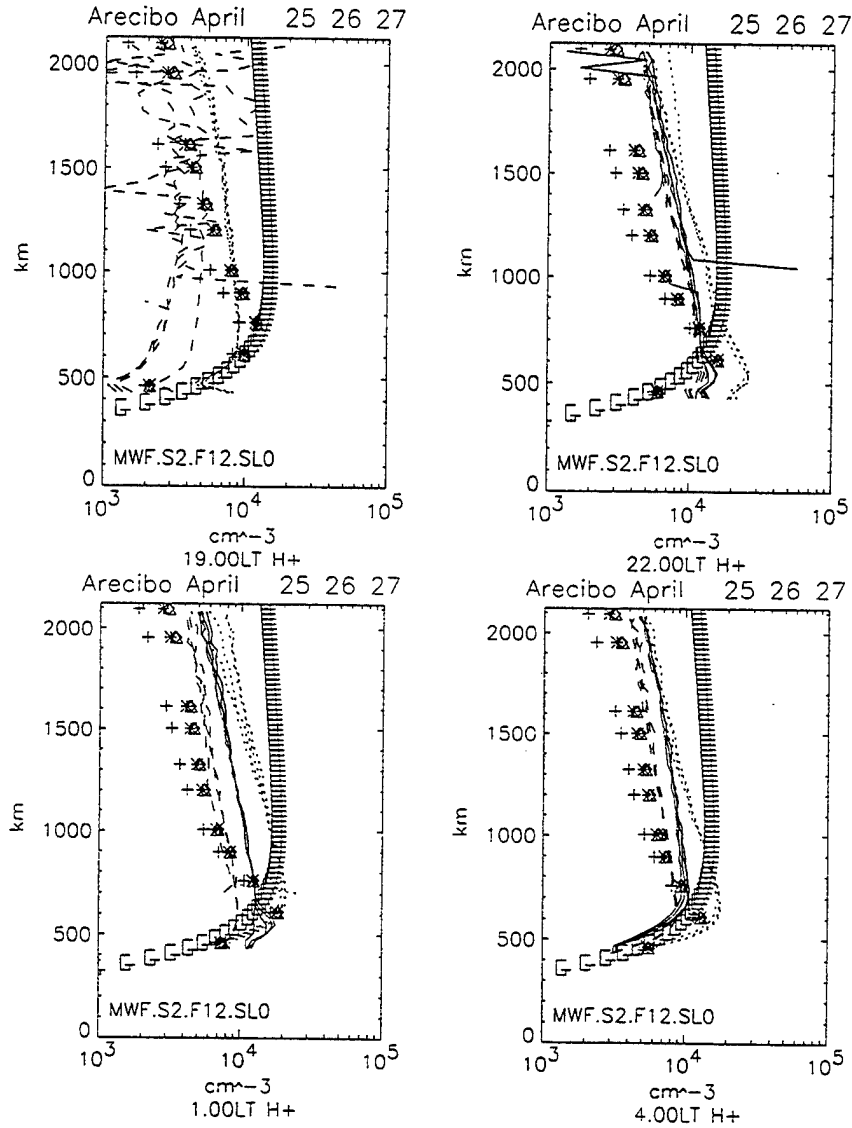
Figure 3. As in Figure 2, but pertaining to H^+ densities. The additional symbols, "G" demonstrate the results of the Gallagher empirical plasmaspheric model.
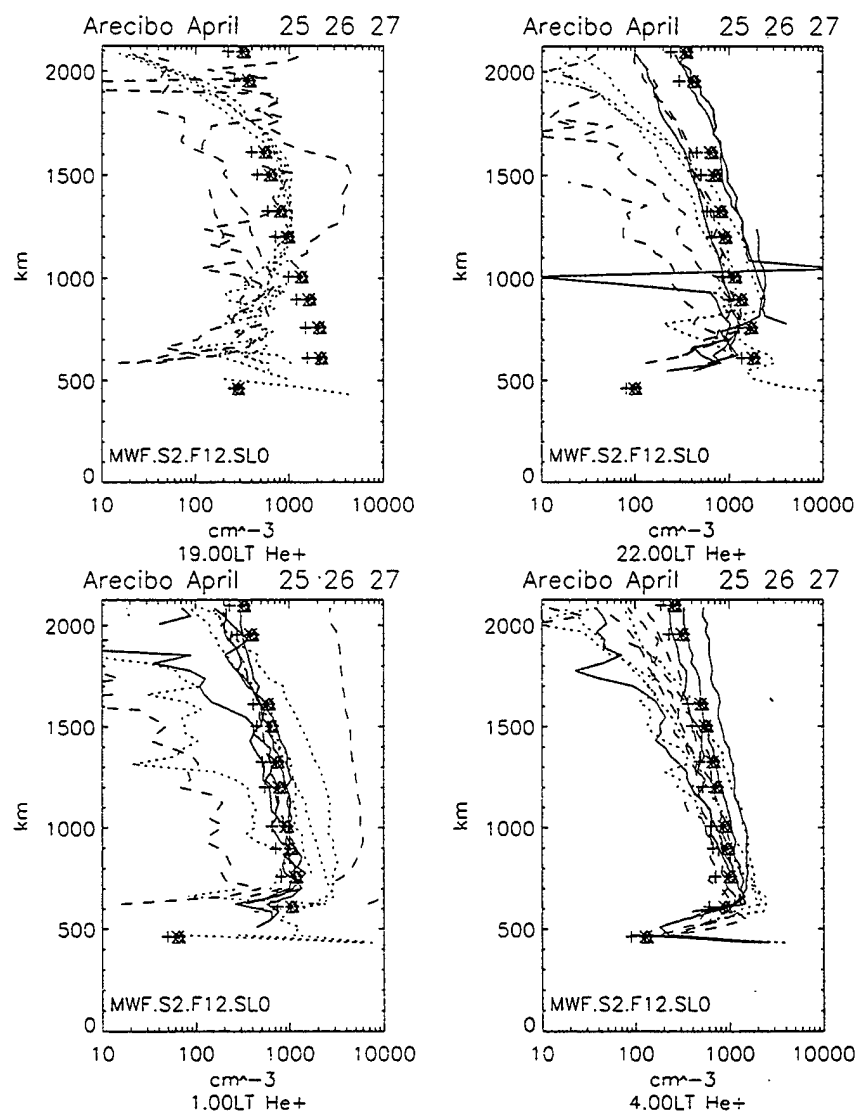
Figure 4. As in Figure 2, but pertaining to He^+ densities.

shell is apparently drifting, while keeping it at the minimum value until it drifts sufficiently upward again to compensate. Equivalently, there is a lower boundary set to the vertical dependence of vertical drifts, with a running measure taken for each fieldline to ensure that no net drift over a wave period is obtained. Testing this approach using null waves (a wave of zero amplitude) has proven successful, though there are numerical differences in densities at the 5% level. This is considered to be the reliability of the method and only wave-related effects of greater than this are regarded as significant in the model.

Subsequently, a series of model runs have been conducted appropriate to conditions where a 16-day periodicity was observed in ionospheric data (Forbes and Leveroni, 1992). Conditions were January, solar maximum (1979), US sector, and in the data some 20-30% (peak-peak) variations were seen in noontime Nmax. The series of model runs were based on several different onset-times for the wavelike variation in the vertical drift pattern, as well as for two different amplitudes, 10% and 25% (20% and 50% peak-peak). It was noted that for 16-day waves, the model results were not sensitive to the onset-time of the wave. Also, the amplitude of the ionospheric effects were not linearly related to the amplitude of the input disturbance.

Figure 5 shows one means of displaying the results. Here, the four panels show variations in Nmax as a function of day in the wave for selected local times (0600LT, 1200LT, 1800LT and 2400LT). Each panel shows the results for a number of different (magnetic) latitudes (-18=solid, -10=dotted, 0=dashed, 10=dot-dashed, 18=dot-dot-dot-dashed). This wave had a peak-peak amplitude of 50%, and an onset time of 1300LT. The following points are noted, both here and in general:

- the corresponding ionospheric responses are largely wavelike

- effects are largest at midnight

- equatorial effects in Nmax are opposite in phase to ΔE (equally, ΔH)

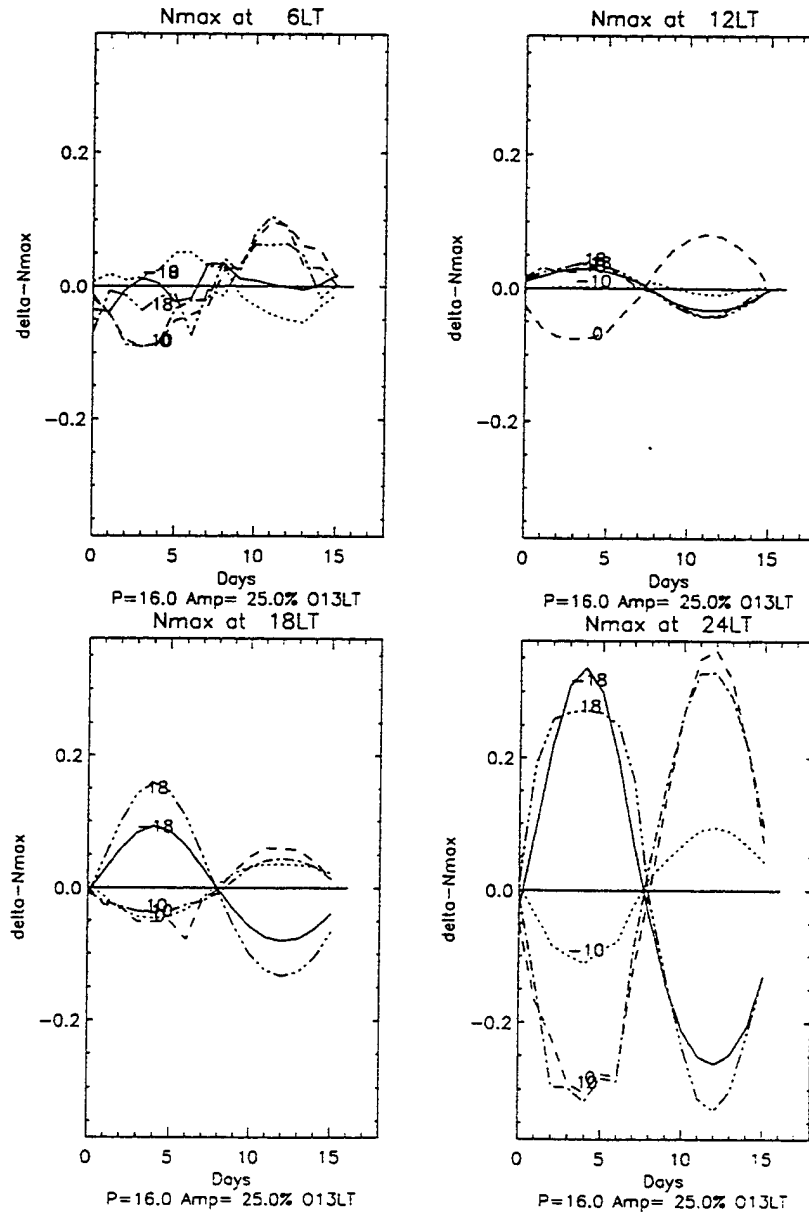Figure 5. Wavelike ionospheric effects in the GTIM when a wavelike **E x B** disturbance is applied. This case was made for January, solar maximum, Huancayo sector conditions, using a 16-day wave and 50% peak-to-peak amplitude. The relative variation in Nmax at selected latitudes (18=solid line,-10=dotted,0=dashed,+10=dot-dashed,+18=dot-dot-dot-dashed) is plotted as a function of the day during the period.

13

- at local times where there is an anomaly crest, effects inside and outside the crests are opposite in sign

- effects in Hmax are much smaller than those in Nmax.

It is seen that equatorial and anomaly effects are the largest. Looking at the noontime Nmax variations in the second panel, it is seen that the amplitude of modeled variations is only 15% rather than the 20-30% seen in the observations. Generally speaking, the modeled variations are smaller. It is the movement of the anomaly crests in the code that gives rise to the larger variations at evening and nighttime periods, and also highlights the variations for noontime Nmax values at the equator.

We next extended the model comparisons to other low latitude ionospheric stations. Ionospheric data (foF2) has been taken from several stations for the same January-April 1979 period originally studied by Forbes and Leveroni (1992). These additional stations are Taipei (magnetic latitude +13), Maui (mag. lat. 20), Rarotonga (mag. lat. -20). Other low latitude stations did not have sufficient data coverage to warrant periodogram analysis. At each of these stations, we compared the amplitude of the observed periodicities at the same 4 Local Times (06, 12, 18, and 24LT) with the model predictions for a similar magnetic latitude.

First, we compared the foF2 variations at Taipei with model results at +10 latitude. Observationally, substantial periodicities are seen in the 18LT and 24LT foF2 values, with significantly smaller variations seen at 12LT, and nothing at 06LT. The model predicts larger variations at 24LT, and smaller at 18LT (albeit at a different longitude sector, implying again that the background vertical drift pattern differs from that assumed in the model, at least in the evening sector), with magnitudes close to those observed at 06LT and 12LT.

Next, we compare the similar results at ±20 magnetic (Maui and Rarotonga) with the

14

model results at ±18 in the model. Observationally, amplitudes are smaller than at other latitudes (at the other sites) and are only significant at 24LT. This is overall the sense of the variations in the model, although again the model amplitudes predicted are significantly larger. This implies that the crests of the equatorial anomaly are close to 18 magnetic in the model, but are somewhat less in the data (Maui and Rarotonga are in the same longitude sector, so this idea is reinforced); the amplitude of wave variations in the model drop very rapidly outside the anomaly crests.

Overall, the model appears to give a good qualitative description of 16-day periodicities in foF2, if one creates a wavelike disturbance along the lines of that proposed by Forbes and Leveroni (1992). Quantitatively, the modeled variations are typically smaller than those observed. Better quantitative agreement would be obtained in general by using vertical drifts in the model obtained from actual measurements, obtained both before and during the disturbance if possible.

4. INVESTIGATING IONOSPHERIC SATELLITE SIGNATURES

The goal of this project was to determine what may be deduced about the dayside ionosphere, primarily the F2-layer peak, given only an in situ electron density measurement, $N_e(840)$. This would enhance the real-time ionospheric monitoring capabilities of the DMSP satellite system.

A modeling study was undertaken using the O^+ GTIM. Ideally, what is sought here is a set of simple relationships that enable reliable estimates of Nmax and Hmax to be made from $N_e(840)$, over a variety of conditions. Important inputs to the model are the specified diurnal variations of both the vertical ion drifts and the meridional neutral wind. In an operational sense, there will be no additional information available on the particular levels of drifts and winds on the day, and thus any proposed method must be made robust with

15

respect to variations in both of these quantities. In general, the level of wind or drift is to be inferred from the in situ density measurements. When either one of the wind or drift were varied, it was evident that correlations existed between Ne(840) and Nmax (or Hmax) that were a function of latitude, local time, season, and level of solar activity.

The important situation, however, is what type of correlations exist in the larger grid of models where both neutral wind level and vertical drift level are varied independently. It became apparent that in many cases, a single relationship existed for all levels, while in a number of other cases, separate relationships were defined for each wind or drift; and in this latter case, that therefore a means of estimating each of the wind or drift will be required.

The procedure for establishing a set of algorithms for deriving Nmax and Hmax (and secondarily, effective wind and effective drift) was a highly interactive one, and was performed as follows:

- for a given season, level of solar activity, and local time, plot Nmax (or Hmax) as a function of Ne(840) at a range of latitudes (each plot covering all wind and drift levels)

- flag those latitudes where no knowledge of wind or drift level is required

- at other latitudes, determine whether separate relationships for either wind or drift level, depending on which looks better to the eye

- determine a latitude where an estimate of wind or drift can be made purely from the value of Ne(840) (specifically, at higher latitudes, vertical drifts have little influence, and thus estimates of wind can be made- similarly at the equator, the vertical drifts dominate and thus Ne(840) usually provides a guide to the effective drift level)

Such a set of coefficients, containing look-up tables for the course of action at each latitude and local time has been developed. Testing of this first set of coefficients was made by generating an additional grid of model GTIM runs, based on effective wind and drift levels offset from those used to develop the coefficients. An error analysis has shown that

the standard deviation of errors is around 5-20% in Nmax, and slightly less in Hmax. The higher figures of standard deviations seem to arise from distributions with a few wildly discrepant points. Ignoring outliers, the standard deviations are typically 5-10% in both Nmax and Hmax. The outliers in turn appear to arise from poor estimates of effective wind or drift, and thus it may be better to base estimates of these on Ne(840) values from more than one latitude in each case. This is more physically sensible as winds and drifts act upon the whole region and not just locally.

5. APPLICATION OF A NEW RAY-TRACING MODEL

A simple profile model was recently developed (Fox, 1994) that is based on the SLIM model, described by Anderson et al. (1987), whereby the profiles derived in a theoretical model at low latitudes were parametrized in terms of Chapman functions for each of the topside and bottomside; Chapman representations in this context are not so much physical descriptions as convenient mathematical descriptions of a basic ionospheric layer shape. However, it differs from SLIM and purely Chapman-like layers in key ways. First, while the topside and bottomside are also described by Chapman layers, the scale heights of the layers are allowed to be height-dependent. This allowed for superior fits to the profiles in the GTIM database. More importantly, the linear dependence with altitude gives rise to analytic expressions for the topside and bottomside density, facilitating use in ray-tracing applications. Second, the nature of the profile fit is that a match is achieved to known values of peak density, peak height and, in terms of summarizing the profile as a whole, slab thickness. The match is achieved by allowing the parameters describing the height variation of the internal scale heights to vary until simultaneous agreement to the peak and summary profile parameters is reached.

The general problem in radiowave propagation is to be able to predict how various

17

frequencies of waves will propagate for a given circuit under given conditions. An operator in the field will want to know which frequencies will work for each circuit and at what elevation angles. Systems already exist that can provide estimates based on climatology but it may not be clear to the operator how any additional real-time observations may be used to help.

For the purposes of ray-tracing through this model we first define the circuit by the transmitter location, receiver location, UT, month and solar flux. In the first instance, we then use the SIMPLI model to come up with climatological profiles for a number (currently, 11) of locations along the circuit. Then, a two-dimensional ray-tracing model is used to determine propagation through this model ionosphere. The propagation is specified by the electron density profiles and their first derivatives, both of which are analytic expressions in the SIMPLI formalism. The profile parameters specified along the circuit are then polynomial fit as a function of ground-distance from the transmitter, so that at any arbitrary distance between the transmitter and receiver, the electron density profile and its slope can be regenerated analytically, as is required for raytracing. Next, over each frequency in the range being considered, the elevation angle required to reach the receiver was determined. Plots of elevation angle versus frequency are the basis for the comparisons presented here.

In the second instance, we wish to set up a method whereby the ionospheric description is updated by some real-time data relevant to the circuit. In the absence of an observational database, the method was tested by using model-driven data, but from an independent model. Here, the Bent model was used, and was run for the same conditions that apply to the given circuit, over the same number of points along the circuit. The "fully updated" model over which ray-tracing is performed is taken from SIMPLI model profile fits to the Bent profiles at the locations along the circuit. This locus of elevation angle versus

frequency defines the ultimate solution (if the ionosphere were completely or correctly specified). Note both the different elevation angles in the true case, as well as the greater range of usable frequencies. It is important to be able to track changes of this nature.

What is being tested here is the ability of the SIMPLI model to assimilate a small amount of data about the circuit and to successfully update radiowave propagation predictions accordingly. The means of testing is to compare the elevation angle loci of different ionospheres where each has resulted from a SIMPLI description using different amounts of "real" (in this case, from the Bent model) data.

Let us demonstrate this concept with an example. Imagine that only the Nmax value at the circuit midpoint is known. Then, the other 10 points along the circuit will have electron density profiles defined by climatological SIMPLI predictions. The midpoint (point 6 out of the 11) will have SIMPLI estimates for the other 6 profile parameters, and the "true" Nmax. Thus, along the circuit, the other 6 parameters will have the same variation as before versus ground distance, while Nmax will have 10 points along the previous curve, and the middle point offset. Two methods of updating the fit of Nmax vs x are:

- performing the same polynomial fit as before through the 10 original and 1 updated points (fitting)

- fitting the 10 points with a polynomial, but offsetting (changing the zeroeth order term) to pass through the midpoint value (shifting).

Successively, the same tests were performed when other parameters (Hmax and slab thickness) and/or specified at other locations (along the circuit) are known. This determined how much data is required for the SIMPLI ray-tracing model to adequately revise its propagation predictions.

We illustrate typical results with the circuit Tx=(30,30), Rx=(20,20), June, F10.7=150, 1200UT, presented in Figure 6. The solid line is the initial guess from SIMPLI
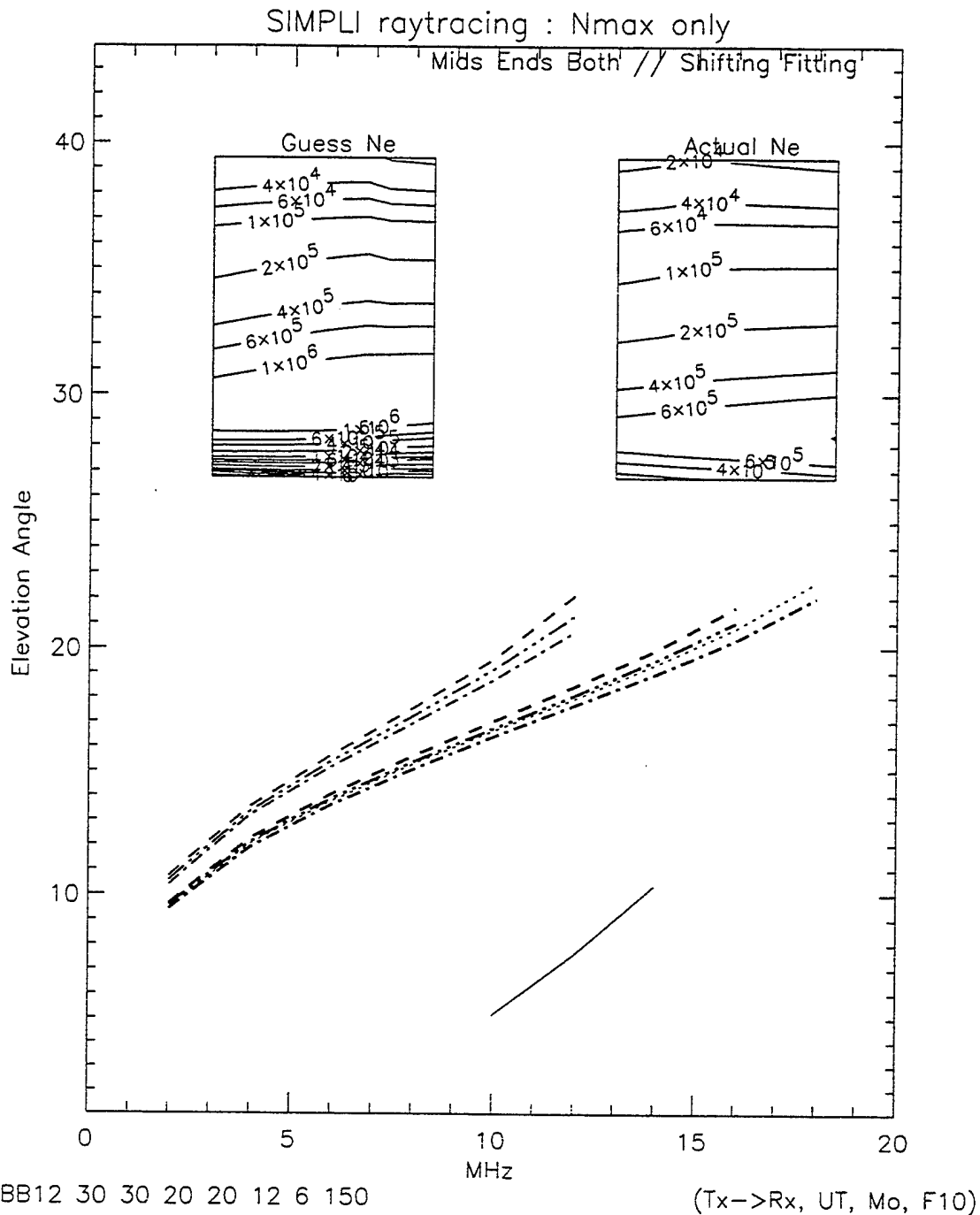
19

Figure 6. The SIMPLI profile model used in raytracing. The solid
line shows elevation angle versus frequency obtained from climatological
estimates (electron density contours in the left insert). The dotted line shows
predictions made from the "ground-truth" ionosphere (right insert). The
upper three lines show predictions based on updating Nmax at the circuit
mid-point and end-points when SIMPLI parameters along the path are shifted
only in the zeroeth order. The lines lying nearest to the dotted line are made
when SIMPLI Nmax values are refit along the path.

for the locus of elevation angle versus frequency for the circuit, based on the ionosphere seen in the left contour plot included in the figure. The dashed line is the locus from the "actual" ionosphere (from the Bent model), seen in the right contour plot, and clearly very different to the SIMPLI climatology in this case. Also seen in this figure are two sets of three different lines, where the thinner lines are derived from the shifting method of updates, and the thicker lines from the fitting method, and where the data used is Nmax from the midpoint (dashed), ends of the circuit (dot-dashed) and all of the above (dot-dot-dot-dashed). In this case, the fitting method is seen to give a fairly good update for the ray propagation, even when only Nmax at the midpoint is known. Using other information (such as Hmax or slab thickness anywhere) did not make any substantive difference- Nmax is sufficient.

This same type of test was peformed over a variety of one-hop circuits over a variety of conditions. In general, the fitting technique provided the more reliable means of updating the SIMPLI model for ray-tracing applications and overall, good results can be achieved when only Nmax at the circuit midpoint is available as an update. Nmax available at either the transmitter or receiver location also provides sufficient information to substantially improve propagation predictions.

6. NEUTRAL DENSITY ANALYSIS

This reporting period has concentrated on the delineation and interpretation of longitudinal structures in the SETA data. These include the "longitude/UT" effect and "longitudinal wave structures", which are discussed separately below.

6.1 Longitude/UT Variation

The existence of a "longitude/UT" effect in the MSIS series of empirical models, which numerically describes the geomagnetic control of high-latitude thermospheric density, suggests that we examine the SETA data for such variations. Since the MSIS models suffer from sparse data coverage at low orbital altitudes and high solar activity, this comparison should be valuable in ascertaining the inadequacies of empirical models under these conditions. This comparison has been a major focus of this year's neutral density contractual activities.

Figure 7 illustrates the time variation of SETA densities, normalized to 200 km and averaged between 20 and 40 degrees latitude, during July 21-26, 1983. MSISE90 density values were calculated for each SETA data point, and averaged in an identical fashion; these values are shown by the dotted line. Note that both the data and model exhibit a repeatable cycle with period of 24 hours or 360 degrees longitude; it is this variation which we refer to as the longitude/UT effect. Note that there is the appearance of the longitude/UT "amplitude" increasing with magnetic activity (a magnetic storm occurred on July 24).

For the present study, we primarily confine ourselves to the magnetically quiet periods during July 20-24, 1983, and December 4-10, 1983. All comparisons between MSIS and SETA correspond to SETA densities normalized to 200 km with the longitude/UT effect removed from the MSIS model. Variations in SETA data which we compare with MSISE90
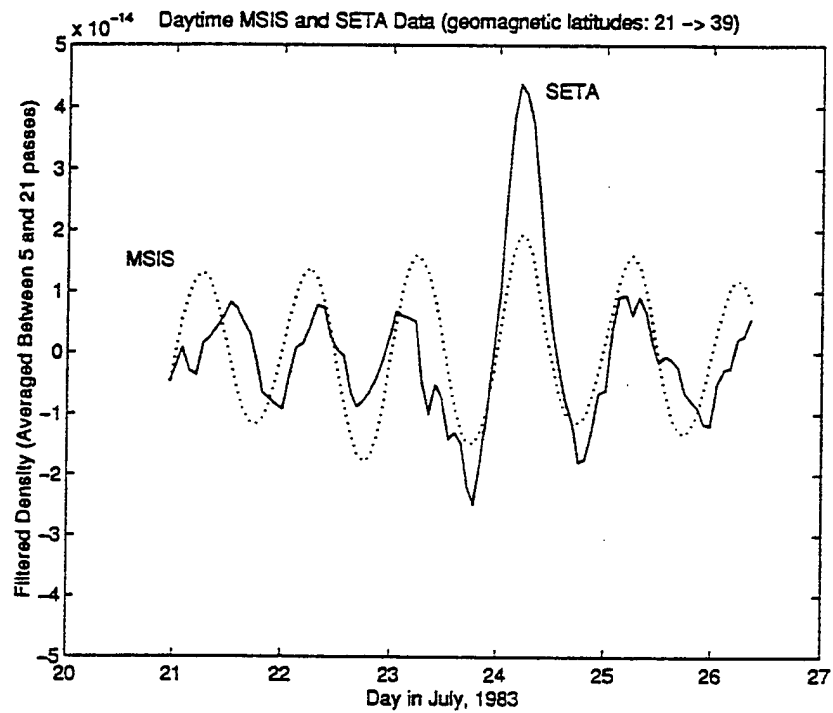
Figure 7. Comparison of SETA and MSISE90 density variations averaged over 20-20 degrees latitude at 1030 LT during July 20-26, 1983.

were extracted as follows. First, the long-term trend was established by performing a 17-orbit running mean. The residuals from this mean were then smoothed (5-orbit running mean) to remove the short-term variations. The result of this process is indicated in Figure 8 for dayside (1030 LT) data averaged over the 0-10° latitude range. The solid line in Figure 8 represents the least-squares fit of a sinusoid with a period of 24 hours (360° in longitude) to the SETA density residuals (circles). The dashed curve represents the corresponding MSISE90 prediction for this period. Note that the amplitude is given in terms of percent variation about the mean density. Figure 8 reveals a distinct periodicity in both the SETA data and MSIS which we are referring to here as the "longitude/UT" effect, although longitude and UT variations cannot be separated or distinguished from the sun-synchronous SETA orbit. The MSIS model exhibits a slightly smaller amplitude and a slight shift in phase with respect to the SETA density oscillation.

Figure 9 summarizes results from the above procedure for all available latitudes for the daytime data during this period. Amplitudes are calculated (a) taking into account the magnetically-active period, and (b) considering only the quiet days. The major model/data discrepancy to be gleaned from this plot is the signficiant latitudinal asymmetry depicted by the SETA data – a factor of 2 to 3 enhancement of the oscillation in the S. Hemisphere; on the other hand, the MSIS model is symmetric about the equator.

An alternative form of depiction is presented in Figures 10 and 11. Here, we provide grey-scale plots of the density comparisons which also take into account the phase (i.e., longitude of maximum) of the "longitude/UT" oscillation. Only the magnetically undisturbed data are used in the fits. These plots also provide comparisons for the nighttime data for the July period, and daytime data for the December period. For the daytime data during July (left-hand panels in Figure 10), SETA and MSIS compare well in phase (i.e., longitude of maximum), but the SETA data suggest the phenomenon to be
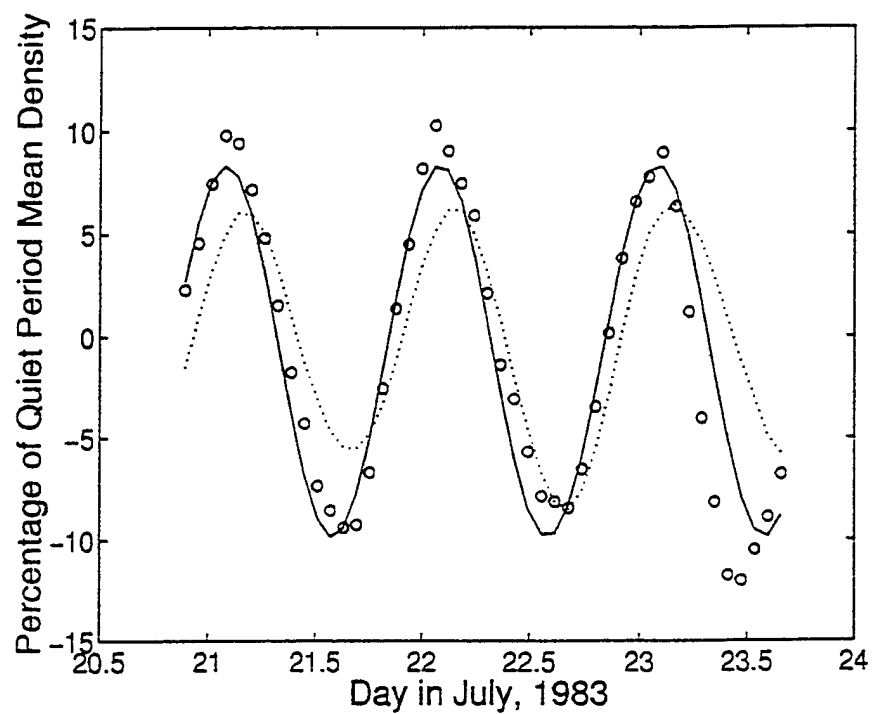
Figure 8. Comparison of "longitude/UT" variation in SETA densities (circles) with MSISE90 (dotted line) during the magnetically quiet period of July 21-23, 1983. Solid line represents least-squares fit of sinusoid to SETA data.
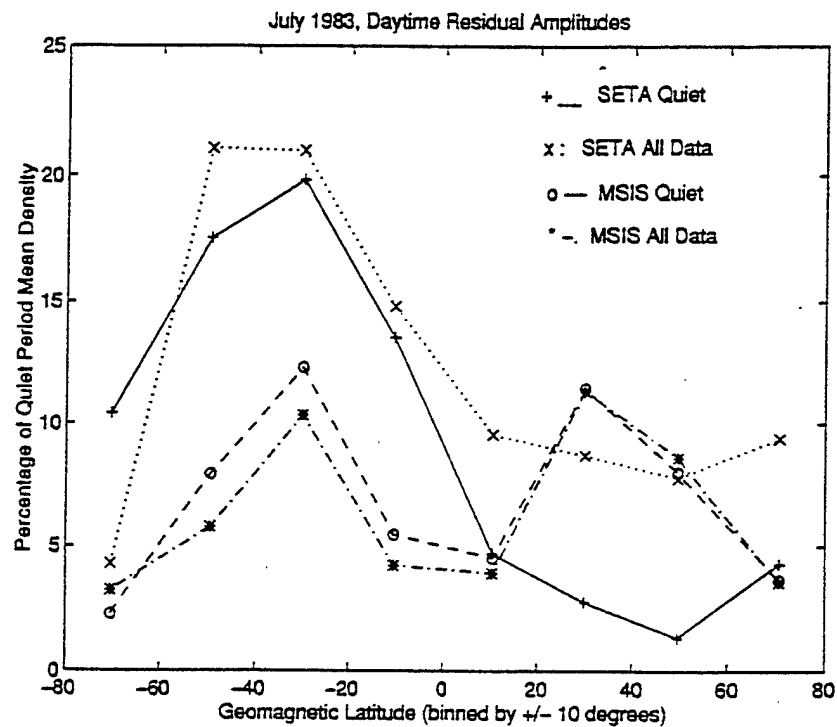
Figure 9. Comparison of amplitudes of "longitude/UT" variation between SETA and MSISE90 as a function of latitude, for daytime data during July 21-23, 1983.
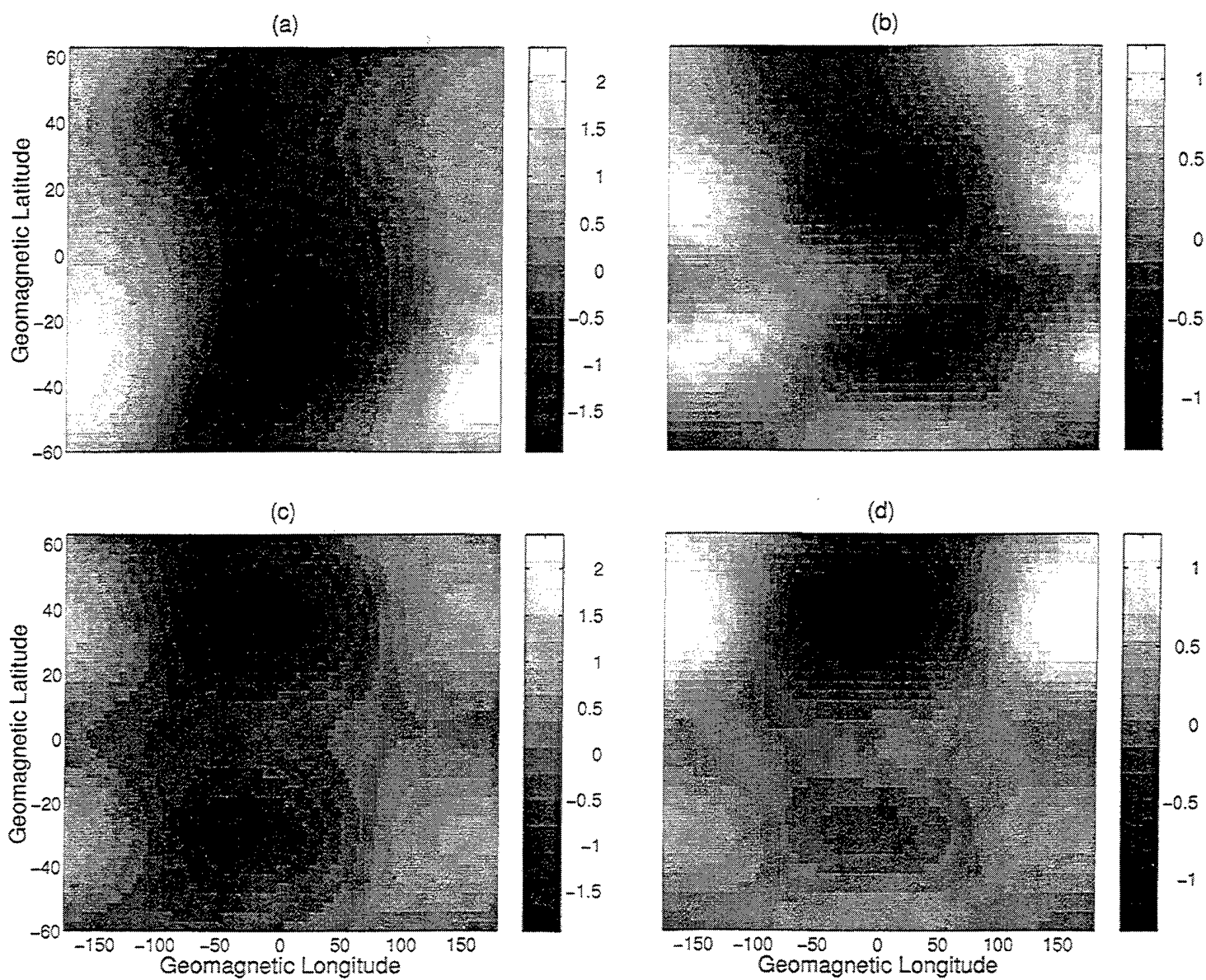
Figure 10. Longitude/UT dependence as revealed by SETA (top) and
MSISE90 (bottom) total mass densities at 200 km during July 21-23, 1983.
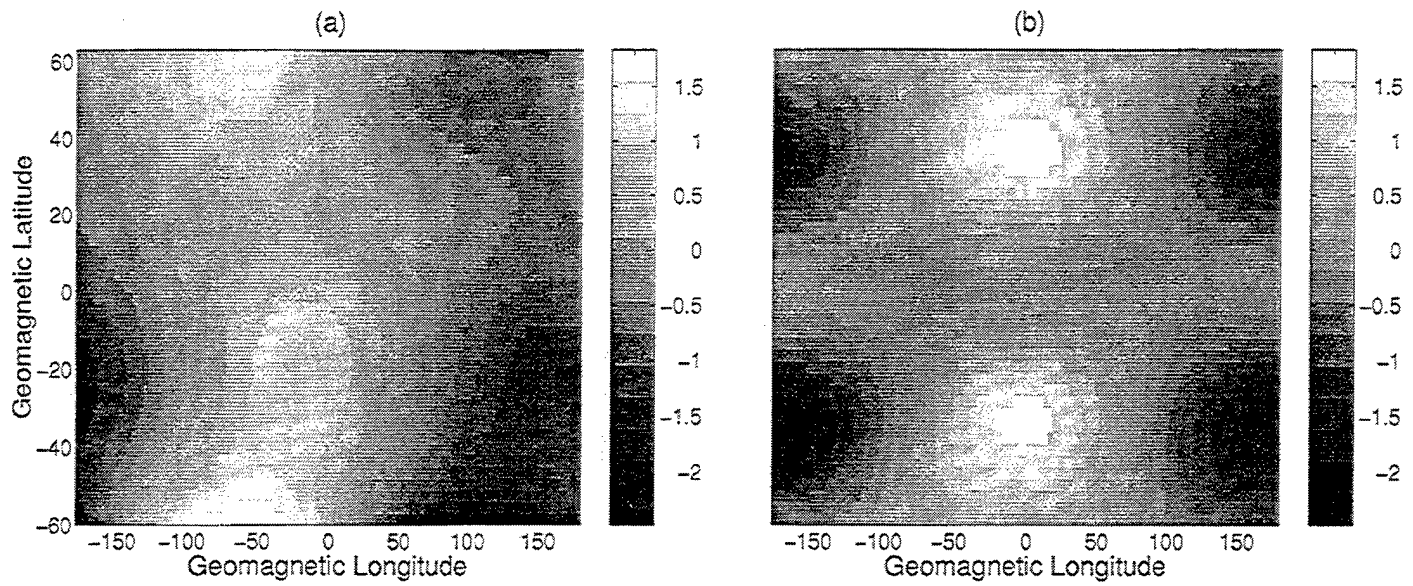Left: daytime (≈1030 LT). Right: nighttime (≈2230 LT).

Figure 11. Longitude/UT dependence as revealed in SETA (left) and MSISE90 (right) daytime ($\approx$1030 LT) total mass densities at 200 km during December 5-10, 1983.

much more robust in the Southern Hemisphere as compared with MSIS. The right-hand panels illustrate the same results, except for nighttime (approx 2230 LT). Here, the converse is true: SETA is more symmetric about the equator, and MSIS is more asymmetric, with much larger perturbations in the Northern Hemisphere. Figure 10 illustrates similar comparisons for daytime data during December 1983, illustrating a very interesting 180 degree shift (for both MSIS and SETA) in the phase (longitude of maximum) of the phenomenon, as compared to the July period. Physical mechanisms underlying the above behaviors, including the seasonal phase shift, are not understood at the present time.

The main conclusion to be drawn from these comparisons is: **There exist significant seasonal/latitudinal differences, in amplitude and phase, between large-scale longitudinal structures revealed by SETA data in comparison to the MSISE90 model during magnetically undisturbed periods; these differences should be incorporated in future empirical modelling efforts in order to improve specifications of thermospheric density for various Air Force applications.**

6.2 Longitudinal Wave Structures

Given the above large-scale trends in the longitude structure of thermospheric density, subsequent efforts have focused on analysis and interpretation of the "residual density variations" superimposed on the large-scale structure. Samples of these residual structures for daytime data during July 20-24, 1983 and December 5-10, 1983, are provided in Figure 12. It is evident that there exist band-like structures extending in the north-south direction. The following describes our efforts to characterize these features quantitatively.

The main difficulty faced in analyzing and interpreting these features is with the space-time sampling inherent from a satellite. The SETA satellites are in sun-synchronous orbits, which means that local time is fixed and the satellite track is nearly at an angle
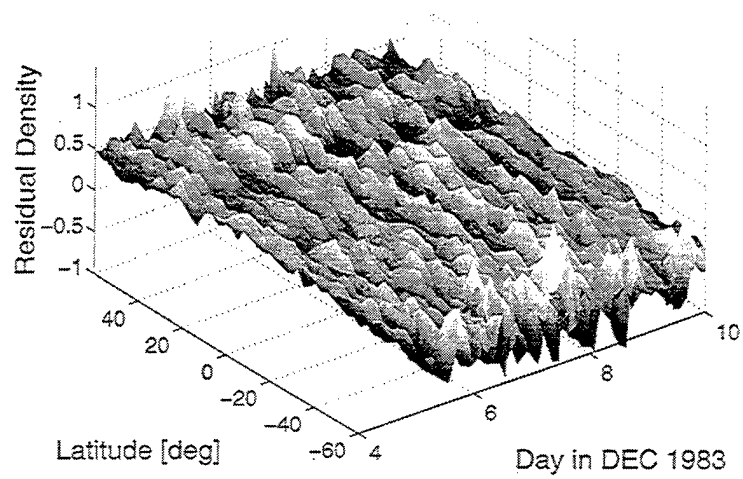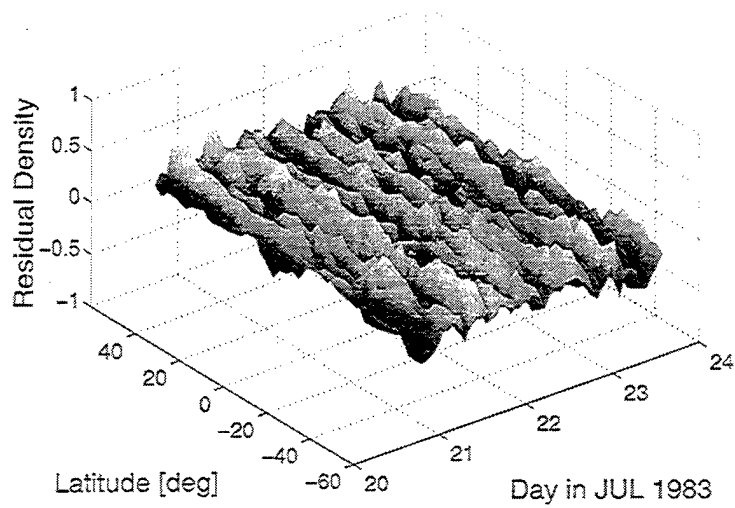
29

Figure 12. Density residuals as a function of latitude and time during magnetically quiet periods during July, 1983, and December, 1983.

of 90° with respect to the equator (actually, the angle is about 83°). The earth (and atmosphere) is thus rotating below the satellite at an approximate rate of 360° longitude per day. Thus, time and longitude are varying continuously, and it is therefore difficult to separate longitude variations from time variations in the atmospheric density. This is especially the case when wave features may in principle be propagating eastward and/or westward with respect to the surface of the earth, as we well know that case to be in the troposphere and stratosphere. Spectral analysis of the data, therefore, leads to some ambiguity in interpretation. The difficulty may be summarized through the relationship

$$k_s = m \pm 1/T$$

where k_s is the zonal wavenumber viewed from the frame of the satellite, m and T are the earth-fixed zonal wavenumber (integer) and period (in days) for a particular oscillation, and the negative (positive) sign corresponds to westward (eastward) propagation. k_s need not be an integer. So, if k_s is found to be 1.33, for instance, from straightforward spectral analysis of the data, this could be interpreted as a westward-propagating m=2 oscillation with T=1.5 days, or an eastward traveling wave with m=1 and T=3 days. Other higher-order combinations are in theory possible, and often it is necessary to either live with the ambiguity, or to deduce the physically correct answer by imposing other constraints.

The most prominent value of k_s derived from spectral analyses of the SETA at different latitudes was a value of 4, with secondary peaks often occurring at 2, 3, 1, and 5. A superposition of spectra for the various latitude bands in the N. Hemisphere for the July daytime data (cf. Figure 12) is illustrated in Figure 13. For $k_s = 2$, for instance, we have as the lowest-order *mathematically* plausible waves (m, T) = (0, 1/2), (2,∞), (1,-1). The first corresponds to a zonally-symmetric semidiurnal tide; the second to a quasi-stationary (i.e., earth-fixed) wave of s=2; the third to an eastward propagating diurnal tide with s=1.
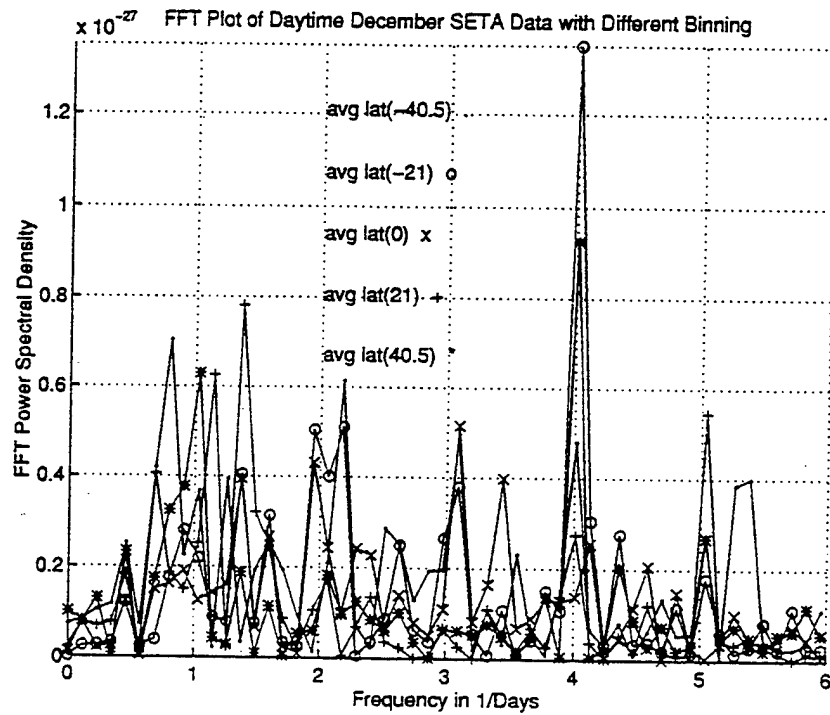
31

Figure 13. Superposition of spectra in different latitude bands, corresponding to the density residuals depicted in Figure 12 for July, 1983.

We eliminate from consideration (m,T) = (1, 1) since this represents a migrating diurnal tide which cannot be detected from a single fixed-local time measurement (in other words, it does not meet the Nyquist criterion). The only plausible choice appears to be the quasi-stationary wave. For $k_s = 4$, we have (m,T) = (4, ∞), (0, 1/4), (5,-1), etc. Again, the migrating semidiurnal tide (2, 1/2) is eliminated from consideration, and there are no known reasons to expect an eastward-propagating wave or a zonally-symmetric 6-hour tide. Our tentative conclusion is that the structures seen in Figure 12, at least those consistent with apparent zonal wavenumbers of 4, 2, 3, 5, and 1 in Figure 13, correspond to earth-fixed features. It is noteworthy that the most prominent wavenumber, $s = 4$, also corresponds to the most prominent wavenumber in the decomposition of land-sea surfaces. This may suggest some relationship with lower-atmosphere physical processes. The thermospheric density amplitude variations associated with these features are about ±2-4%.

We are led to the following conclusion: **Longitudinal wave structures of order ±2-4% exist in thermospheric density, with apparent earth-fixed zonal wavenumbers ranging between 1 and 5. Zonal wavenumber 4 appears to play an important role. Analyses of additional geophysical periods, perhaps using more sophisticated spectral analyses techniques, may lead to improved quantification and interpretation of this phenomenon.**

REFERENCES

Anderson, D. N., A theoretical study of the ionospheric F-region equatorial anomaly, I. Theory, *Planet. Space Sci.*, **21**, 409, 1973.

Anderson, D. N., M. Mendillo and B. A. Herniter, A semi-empirical low-latitude ionospheric model, *Radio Sci.*, **22**, 292, 1987.

Brace, L. H. and R. F. Theis, Global empirical models of ionospheric electron temperature in the upper F-region and plasmasphere based on in situ measurements from the Atmospheric Explorer-C, ISIS 1 and ISIS 2 satellites, *J. Atmos. Terr. Phys.*, **43**, 1317, 1981.

Forbes, J. M. and S. Leveroni, Quasi 16-day oscillations in the ionosphere, *Geophys. Rev. Lett.*, **19**, 981, 1992.

Fox, M. W., A simple, convenient formalism for electron density profiles, *Radio Sci.*, **29**, 1473, 1994.

Fox, M. W., X. Q. Pi and J. M. Forbes, New applications of the Phillips Laboratory theoretical ionospheric model and studies of neutral density waves, *Phillips Laboratory* Hanscom AFB, MA 01731-3010, 1994, PL-TR-94-2161, ADA284663.